HHS Public Access

Author manuscript

Magn Reson Med. Author manuscript; available in PMC 2019 January 01.

Published in final edited form as:

Magn Reson Med. 2018 January ; 79(1): 394–400. doi:10.1002/mrm.26643.

A constrained slice-dependent background suppression scheme for simultaneous multi-slice pseudo-continuous arterial spin labeling

Xingfeng Shao[1], **Yi Wang**[2], **Steen Moeller**[3], and **Danny JJ Wang**[1,*]

[1]Laboratory of FMRI Technology (LOFT), Mark & Mary Stevens Neuroimaging and Informatics Institute, Keck School of Medicine, University of Soutern California, CA 90033, United States

[2]MR Clinical Science, Philips Healthcare, Gainesville, FL 32608, United States

[3]Center for Magnetic Resonance Research, University of Minnesota, Minneapolis, MN 55455, United States

Abstract

Purpose—To present a constrained slice-dependent (CSD) background suppression (BS) scheme in 2 dimensional (2D) arterial spin labeling (ASL) using simultaneous multi-slice (SMS) acquisition with blipped-CAIPIRINHA (controlled aliasing in parallel imaging results in higher acceleration).

Methods—BS for 2D acquisition is challenging due to multiple nulling points required for sequential slice readout. CSD BS exploits SMS technique to reduce the readout duration and employs slice-dependent pre-modulation pulses to achieve BS across slice groups. The proposed scheme was evaluated by in vivo brain experiments at 3T with multi-band (MB) acceleration factors up to four. The utility of CSD BS was demonstrated through comparison against standard 2D acquisitions as well as 3D BS pseudo-continuous ASL (pCASL).

Results—An average of 95% background signal reduction was achieved with CSD BS. As a result, temporal signal-to-noise ratio (t-SNR) increased 48.2%/39.9%/36.9%/36.0% and spatial SNR increased 132.5%/80.0%/63.5%/54.2% in CSD BS MB-1/2/3/4 scans respectively. Whole brain coverage was achievable with CSD BS pCASL with MB-4 that yielded comparable spatial SNR as 3D BS pCASL.

Conclusion—The proposed CSD-BS scheme for 2D SMS pCASL offers a promising approach for effective suppression of background signals across a wide range of T1s to achieve whole-brain perfusion imaging.

Keywords

Background suppression (BS); Arterial spin labeling (ASL); Simultaneous multi-slice (SMS); Controlled aliasing in parallel imaging results in higher acceleration (CAIPIRINHA)

[*]**Corresponding Author:** Danny JJ Wang, Phd, MSCE, Laboratory of FMRI Technology (LOFT), Mark & Mary Stevens Neuroimaging and Informatics Institute, Keck School of Medicine, University of Southern California (USC), jwang71@gmail.com, Phone: 323-442-7246.

Introduction

Due to the small fractional signal of labeled blood, arterial spin labeling (ASL) is sensitive to noise induced by motion and system instabilities. Reduction of the background signal in an ASL study can greatly suppress the signal fluctuation and increase temporal signal-to-noise ratio (t-SNR) (1–5). The idea of background suppression (BS) was first introduced by Dixon to suppress brain tissue signals in projection angiography using several inversion pulses following a pre-saturation of the whole imaging volume (6).

Background suppression is optimal for 3D imaging due to the single excitation of the whole volume. However, fast 3D acquisitions commonly used for ASL, such as gradient-and-spin echo (GRASE), suffer from spatial blurring due to the modulation of k-space signals by the transverse (T2) relaxation during the relatively long readout time. Consequently, multi-shot segmented 3D acquisitions are required at present and recommended by the ASL white paper which limit the temporal resolution of ASL scans and make the data susceptible to motion and physiological fluctuations (1). Another promising technology in ASL is simultaneous multi-slice (SMS) or multiband (MB) imaging, which simultaneously excites multiple slices and recovers each slice with parallel imaging techniques. Compared to standard 2D ASL, MB ASL can reduce T1 relaxation effect of the label, improve spatial coverage and resolution with little penalty in SNR (except for the coil geometry factor or g-factor) (7–9). However, existing MB ASL techniques are still suboptimal for the background suppression technique since multiple MB excitations are required and the background signal recovers with sequential slice acquisitions. As a result, the t-SNR of MB-EPI ASL is inferior to that of 3D BS GRASE ASL (10).

Applying BS for 2D imaging has not been studied extensively due to the difficulty of choosing the optimal nulling point. A more common approach is to optimize the timing of the BS pulses to suppress gray matter and white matter signals in the first imaging slice as demonstrated in (11,12). Such a BS scheme with single whole volume saturation (WVS-BS) increases t-SNR as compared to that of a non-BS sequence. However, a t-SNR reduction in later EPI readout is still observable and could be attributed to the recovered background signal. St. Lawrence *et. al.*, proposed a multi-slice version of ASSIST (Attenuating the Static Signal in Arterial Spin Tagging) technique to maintain the background signal beyond the first null point by applying additional global inversion pulses between slice acquisitions (2), however those inversion pulses could increase specific absorption rate (SAR) of RF power as well as prolong the acquisition time. In this study, we propose a novel constrained slice-dependent BS (CSD-BS) scheme for 2D multi-slice pseudo-continuous ASL (pCASL) with SMS-EPI acquisition, to suppress background signal across a wide range of T1s. Each group of simultaneously excited slices are pre-modulated separately and then re-nulled when excited for each group of slices after two global inversions. The proposed CSD-BS scheme was optimized for timing by numerical simulation and evaluated by in vivo studies.

Methods

Theoretical Calculation

The timing of the proposed CSD-BS scheme for 2D SMS-EPI pCASL sequence is illustrated in Figure 1 (a). The longitudinal magnetization, M_Z, in each group of SMS slices (represented by the same color) is pre-modulated and then excited simultaneously with composite multiband RF pulses. Two spatially non-selective hyperbolic secant (HS) pulses with a duration of 10.24 ms are implemented as global inversion pulses during the post-labeling delay (PLD) to modulate M_Z in all imaging slices for precise nulling of background signals without disturbing inflowing blood signal. Specific constraints can be imposed on the proposed CSD-BS scheme depending on the experimental condition. For the present study, we constrained the two non-selective HS inversion pulses to be applied during the PLD without interrupting the labeling/control pulse train. Note this constraint can be relaxed for short PLDs as will be shown below.

Figure 1 (b) shows an example of 2 imaging slices with the trajectories of normalized M_Z background tissue. Slice-dependent pre-modulations allow each slice group experience a specific timing scheme and the nulling point can be pre-specified by adjusting the flip angles (FAs) of pre-modulation RF pulses. According to (6,13), the normalized magnetization for imaging slice group i and a specific longitudinal relaxation time $T_{1,j}$ can be expressed as:

$$M_{Z,i}(T_{1,j})=(M_{Z,i}(0)-1)\exp(-\frac{Q_i+(i-1)\tau_{\text{acq}}}{T_{1,j}})+2\exp(-\frac{\tau_{\text{inv},1}+(i-1)\tau_{\text{acq}}}{T_{1,j}})-2\exp(-\frac{\tau_{\text{inv},2}+(i-1)\tau_{\text{acq}}}{T_{1,j}})+1 \quad [1]$$

where i is the slice group index, $Q_i = (S - i + 1)\tau_{\text{pre}}$+LD+PLD, S is the total number of slice groups, τ_{pre} is duration of pre-modulation, LD and PLD represents labeling duration and post-labeling delay respectively, τ_{acq} is the acquisition time of a single EPI readout, and $\tau_{\text{inv},1}$/$\tau_{\text{inv},2}$ are the time interval between the first/second inversion pulse and the SMS-EPI readout, respectively. $M_{Z,i}(0)$ is the initial longitudinal magnetization determined by the FA α_i of pre-modulation pulses:

$$M_{Z,i}(0)=M_{0,i}(T_{1,j})\cos(\alpha_i) \quad [2]$$

where $M_{0,i}(T_{1,j})$ is the longitudinal magnetization of ith slice determined by T1 relaxation during the interval between pre-modulation and the readout excitation in previous TR. Estimation of BS timing parameters, including the modulation FA ($\mathbf{A}$ =[α_i]) and inversion times ($\mathbf{T}_{\text{inv}}$ =[$\tau_{\text{inv},1}$, $\tau_{\text{inv},2}$]), can be treated as a nonlinear optimization problem to minimize total residual signal, expressed as the squared sum of background signals across a range of T1 values for all imaging slices:

$$\underset{\mathbf{A}\in[0,\pi],\mathbf{T}_{\text{inv}}\in\tilde{T}_{\text{inv}}}{\operatorname{argmin}} \left(\sum_{i=1}^{S}\sum_{j=1}^{N} M_{Z,i}(T_{1,j})^2\right) \quad [3]$$

where N is the number of target T1 values. Those parameters were optimized using Trust-Region-Reflective Optimization implemented in MATLAB (MathWorks Inc., Natick, MA) (14,15). Constraints were placed on timing parameters to ensure no pulse falls into the labeling module: $\tilde{T}_{\text{inv}}=[0, \text{PLD}]$. To sufficiently cover T1 values in brain, residual background signals for T1s ranging from 700 to 1400ms with a step size of 25ms, were equally weighted in the optimization.

MRI Experiments

Four healthy volunteers (age = 31±9 years, 3 male) were scanned on a Siemens 3T Prisma scanner (Erlangen, Germany) using a 32-channel head coil after they provided informed consent according to a protocol approved by the local Institutional Review Board (IRB). The optimized CSD-BS scheme was implemented for a SMS-EPI pseudo-continuous ASL (pCASL) sequence with MB factors of 1, 2, 3, and 4 respectively. Imaging parameters for the SMS-EPI sequence were: FOV=224mm, resolution=3.5 × 3.5 ×5mm^3, slice gap=1mm, ascending slice ordering, bandwidth=3004Hz/pixel, echo spacing=0.45ms, TE=12ms, TR=4500ms, phase partial Fourier=6/8, FA=90°, LD=1500ms, PLD=1800ms, τ_{acq}=45ms and 40 acquisitions with a total scan time of 3min. The labeling plane was placed 90mm below the center of the imaging volume. Six slice groups were acquired sequentially where each slice group included 1/2/3/4 slices with MB factor-1/2/3/4 respectively. The inter-slice gaps between simultaneously excited slices were 36 mm for MB factor-2/3/4. The blip-CAIPI technique was applied with a relative FOV shift along the phase encoding direction for simultaneously excited slices (16). A single-band (SB) reference scan was acquired before each SMS acquisition and the SMS images were reconstructed off-line using slice-GRAPPA algorithms with a kernel size of 5x5 and sliceblocking to reduce leakage artifacts (16,17). For clarification, both SB and MB-1 refer to the acquisition without SMS acceleration. SMS pre-modulation was implemented by combining phase-modulated sinc RF pulses, which were identical as excitation pulses for EPI readout, with optimized FAs derived from Eq. [3]. Each pre-modulation MB RF pulse had 2.56ms duration and time bandwidth product of 5.2, followed by a 0.68ms spoiler gradient along Y-axis. A 1mm slice gap was added to minimize potential slice cross-talk due to large pre-modulation FAs.

For quantitative comparison, a WVS-BS scheme with whole volume pre-saturation was applied with a standard 2D EPI pCASL sequence on four volunteers. Imaging parameters including slice position of the EPI sequence were kept the same for the two BS schemes, while a whole volume saturation pulse with a fixed FA of 90° was employed for WVS-BS and the timing of the two inversion pulses was optimized for precise nulling of the first slice. The mean signal and t-SNR of each slice were calculated and compared between WVS-BS and CSD-BS scans.

In addition, a 3D segmented GRASE pCASL sequence with optimized WVS-BS was performed on four healthy volunteers for comparison with SMS-EPI pCASL. The imaging parameters were: FOV=224 mm, 100% phase-sampling, resolution=3.5 × 3.5 × 3mm^3, slices per slab=48, slice oversampling=10%, bandwidth=2604Hz/pixel, echo spacing=0.40ms, turbo factor=14, segments=4, TE=30.78ms, TR=4500ms, centric ordering, refocusing FA=120°, label/control duration=1500 ms, PLD=1800ms, 10 acquisitions with a total scan time of 3min. The labeling plane was placed 90 mm below the center of imaging volume. The slab thickness of 3D GRASE was 144mm which was sufficient for whole brain coverage. A similar volume coverage of 143mm was achieved with MB-4 SMS EPI. However, the slice thickness was doubled in SMS-EPI with 5-mm slice thickness and 1-mm inter-slice gap as compared to that of 3D GRASE.

Quantitative Analysis

All quantitative measurements were performed on the common six slices shared by all SMS acquisitions (8). The average signal intensity was compared between skull removed BS and non-BS images to evaluate the effectiveness of background suppression. Pixel-wise t-SNR was calculated in gray matter as the ratio of the mean signal to the standard deviation (SD) of the perfusion time series within each pixel (5,20). Even and odd numbered perfusion images were averaged and then added/subtracted to produce the sum/difference images respectively. The spatial SNR was evaluated in gray matter as the ratio of the mean signal in the sum image divided by the SD of signals in the difference image as reported by (10,21). The purpose of difference images between even and odd perfusion images was to eliminate noise contributions from brain physiology. For calculations of both tSNR and spatial SNR, gray matter masks were generated from a product T1-weighted MP-RAGE sequence using SPM12 (Wellcome Trust Center of Neuroimaging, London, UK). For comparison of SNR between 3D GRASE and SMS-EPI pCASL, even and odd slices were summed in the 3D GRASE scan to match the same slice positions in the SMS-EPI scan.

Results

Simulation and in vivo results of CSD-BS scheme

For the imaging parameters employed for the in vivo pCASL scans (LD = 1500ms, PLD = 1800ms), the optimized parameters for CSD-BS scheme were: $\mathbf{A}$ =[0, 23, 70, 138, 180, 180]° and $\mathbf{T}_{inv}$ =[1545, 284] ms. On average, the background signals across six slices were suppressed to 4.3±2.9% of original intensities using the proposed CSD-BS scheme based on simulation for equally weighted T1 values ranging from 700 to 1400ms. However, increased residual background signals were observed for edge slices and shorter T1 values, as shown in supporting Figure S1. The matlab stimulation program for the CSD-BS scheme can be downloaded at http://www.loft-lab.org/index-5.html

Figure 2 shows control images (first row), perfusion weighted images (second row) and t-SNR maps (third row) of a representative slice acquired with non-BS SB and CSD-BS MB-1/2/3/4 scans. Note the slice acquisition order in MB-1/3 and MB-2/4 scans were different for the common central 6 slices and thus the contrast for displayed control images was not identical, as demonstrated in Figure 2 (b). On average, the background signal of the

common six slices was suppressed to 6.1 ± 0.3 %, 5.7 ± 0.4%, 5. 9 ± 1. 0% , and 5.6 ±0.9% (mean±SD across four subjects) of original intensities in CSD-BS MB-1/2/3/4 images respectively. T-SNR maps showed t-SNR increase in CSD-BS scans while slight perfusion signal and t-SNR drop could be observed with increased MB-factor potentially caused by a higher *g*-factor.

Figure 3 shows the mean t-SNR and spatial SNR from four volunteers. Mean tSNR in gray matter was 1.45±0.18, 2.16±0.23, 2.04±0.21, 2.00±0.14, 1.98±0.07 and the spatial SNR was 2.55±0.76, 5.93±1.29,4.59±1.43, 4.17±0.25, 3.94±0.78 for non-BS SB and CSD-BS MB-1/2/3/4 respectively. Compared to standard 2D EPI pCASL without BS, the proposed CSD-BS scheme increased mean tSNR by 48.2%, 39.9%, 36.9% and 36.0% and spatial SNR by 132.5%, 80.0%, 63.5% and 54.2% in MB-1/2/3/4 data respectively, which indicates a more stable perfusion signal in both spatial and temporal domains with BS acquisitions.

Comparison of CSD-BS and WVS-BS schemes

The timing of the two inversion pulses was optimized for WVS-BS schemes as: $\mathbf{T}_{inv}$ =[1514, 346] ms. Figure 4 (a) shows the slice-wise signal of control images with two BS schemes from one representative subject. Although the signal from the first imaging slice was effectively nulled using WVS-BS technique, image intensity of the following slices experienced magnetization recovery due to T1 relaxation. In contrast, the proposed CSD-BS presented more effective background signal suppression across slices, as demonstrated in Figure 4 (a), though no single nulling point was specifically defined. Quantitatively, the CSD-BS scheme suppressed the signal intensities for the six imaging slices to 4.1%, 3.0%, 3.3%, 5.2%, 8.5% and 11.7% respectively, as compared to 2.4%, 5.0%, 7.8%, 10.9%, 14.1% and 17.2% using WVS-BS. Figure 4 (b) shows the t-SNR maps from CSD-BS and WVS-BS sequences respectively. Intuitively, both BS schemes could effectively improve the t-SNR compared to that of non-BS scans. However, the presented CSD-BS outperformed the WVS-BS especially in later slices due to a lower level of signal suppression. On average, the proposed CSD-BS scheme yielded 37.5% lower suppressed signal intensity and 11.7% higher mean t-SNR compared to those of WVS-BS scans respectively.

Comparison of SMS pCASL with CSD-BS and 3D GRASE pCASL

Figure 5 shows the central 16 slices of perfusion weighted images acquired with 3D segmented GRASE and SMS-EPI MB-4 sequences. The t-SNR/spatial SNR in gray matter from 24 slices were 4.05±1.31/3.83±0.57 for 3D GRASE and 2.04±0.07/4.07±0.76 for SMS-EPI scans with CSD-BS. T-SNR was 98.5% higher but spatial SNR was 5.9% lower in 3D GRASE scans compared to 2D MB-4 EPI scans respectively. Compared to a 2 to 3-fold difference in tSNR and spatial SNR between BS 3D and non-BS 2D ASL scans reported in literature (22), proposed CSD-BS scheme yielded relatively comparable spatial SNR values as those of 3D BS GRASE pCASL. Compared to 3D GRASE images that display spatial blurring along partition encoding direction, reduced blurring was observed in SMS-EPI images, as illustrated in three enlarged regions in Figure 5.

Discussion

ASL scans incorporating BS schemes have markedly improved t-SNR, which is of particular value in clinical ASL scans where scan times must be kept as short as possible to achieve adequate diagnostic quality of perfusion images (1). About 95% of background signal reduction has been achieved for SMS-EPI pCASL with the proposed CSD-BS scheme. As a result, t-SNR of perfusion images has increased significantly, ranging from 36.0% in MB-4 to about 1.5-fold in MB-1 scans, as compared to non-BS scans. This study also demonstrated that CSD-BS could be beneficial for spatial SNR due to suppressed background noise and signal fluctuation.

More inversion pulses offer a higher degree of freedom for the BS scheme while shorter readout duration is beneficial for suppressing the signal fluctuation, both leading to greater BS effects. Previous studies have shown a 9% perfusion signal loss at 3T with just one BS inversion pulse (23) and the loss of labeling efficiency as well as the concern of SAR discouraged the use of a larger number of inversion pulses for BS. Given these considerations, two inversion pulses were employed in the present study as a balance between achieving sufficient labeling efficiency and minimizing signal fluctuations. Though two inversion pulses may not achieve a high-level of background suppression (~1%) compared to four or more inversions as demonstrated by earlier studies (3,4,13), a slightly higher signal intensity could be beneficial for separating aliased SMS signal as well as for intensity based motion correction.

The existing implementation of CSD-BS with SMS pCASL was based on typical parameters recommended by the ASL white paper (e.g. 1500ms LD and 1800ms PLD) (1). We chose to impose the constraint and keep the LD “intact” by the BS pulses for the sake of simplicity and concern of potential loss of efficiency by inserting BS pulses in the labeling/control pulse train. Both constrained and unconstrained CSD-BS scheme, which allows inversion pulses to fall into LD, was simulated for LD and PLD ranging from 300ms to 3000ms at a step of 150ms. The results showed that constrained scheme is not necessary when PLD is longer than 30% of the LD (e.g. 1500ms LD and >450ms PLD) while background signal can be consistently suppressed to 4%-7% of its original signal intensity both with and without the constraint (see supporting Figure S2). However, for PLDs shorter than 30% of the LD, the constraint of intact LD need to be relaxed in order to achieve a high degree of BS.

Though this work only employed an imaging protocol with six slices, CSD-BS can be easily extended for a greater number of slices or a wider T1 range. The pre-modulation pulses will slightly prolong the total acquisition time (3.24ms per slice group), accounting for less than 1% in one measurement without affecting the ASL contrast. Large pre-modulation FAs may potentially cause slice cross-talk, and SLR pulse design for MB excitation may be employed in the future (18,19). One potential drawback of CSD-BS is the variation of signal intensity and contrast across slice groups, as shown in Figure. 2. This signal variation arises from different evolutions of magnetization of each slice group and can be minimized by keeping the image readout duration as short as possible. Minimal echo spacing and TE were chosen for the current protocol and total readout duration for the six slice groups was 246 ms. On the other hand, longer T1 values (>1000ms) will generally dampen signal variations across

slice groups based on our simulation (see supporting Figure S1). Therefore CSD-BS may potentially benefit at high fields and for longer T1 values beyond the simulation range (700–1400ms). In the future, the proposed CSD-BS SMS-EPI scheme may be further improved by additional approaches such as reversing or shifting the excitation order of SMS slice groups across measurements.

The combination of CSD-BS with 2D SMS-EPI pCASL offers an appealing alternative to the segmented 3D pCASL technique. The advantages of 2D SMS-EPI pCASL include single-shot whole brain coverage without potential spatial blurring, while segmented 3D GRASE pCASL may be sensitive to head motion between segmented acquisitions which is challenging for retrospective motion correction. Currently, the slice thickness of our existing SMS-EPI pCASL with CSD-BS (5mm) is still larger than that of the segmented 3D GRASE pCASL (3mm). Future work includes improving the spatial resolution of SMS-EPI pCASL with higher MB factors.

Conclusions

We proposed a novel CSD-BS scheme for 2D SMS pCASL to achieve effective BS across sequentially acquired slices and thereby improving temporal stability for ASL. CSD-BS based 2D SMS pCASL offers an alternative to 3D BS pCASL with segmented readout.

Supplementary Material

Refer to Web version on PubMed Central for supplementary material.

Acknowledgments

This research was supported by the National Institute of Health (NIH) Grants UH2-NS100614, R01-EB014922 and P41-EB015894.

Reference

1. Alsop DC, Detre JA, Golay X, Gunther M, Hendrikse J, Hernandez-Garcia L, Lu H, MacIntosh BJ, Parkes LM, Smits M, van Osch MJ, Wang DJ, Wong EC, Zaharchuk G. Recommended implementation of arterial spin-labeled perfusion MRI for clinical applications: A consensus of the ISMRM perfusion study group and the European consortium for ASL in dementia. Magn Reson Med. 2015; 73(1):102–116. [PubMed: 24715426]
2. St Lawrence KS, Frank JA, Bandettini PA, Ye FQ. Noise reduction in multi-slice arterial spin tagging imaging. Magn Reson Med. 2005; 53(3):735–738. [PubMed: 15723412]
3. Garcia DM, Duhamel G, Alsop DC. Efficiency of inversion pulses for background suppressed arterial spin labeling. Magn Reson Med. 2005; 54(2):366–372. [PubMed: 16032674]
4. Maleki N, Dai W, Alsop DC. Optimization of background suppression for arterial spin labeling perfusion imaging. MAGMA. 2012; 25(2):127–133. [PubMed: 22009131]
5. Bennett CM, Miller MB. How reliable are the results from functional magnetic resonance imaging? Ann N Y Acad Sci. 2010; 1191:133–155. [PubMed: 20392279]
6. Dixon WT, Sardashti M, Castillo M, Stomp GP. Multiple inversion recovery reduces static tissue signal in angiograms. Magn Reson Med. 1991; 18(2):257–268. [PubMed: 2046511]
7. Feinberg DA, Moeller S, Smith SM, Auerbach E, Ramanna S, Gunther M, Glasser MF, Miller KL, Ugurbil K, Yacoub E. Multiplexed echo planar imaging for sub-second whole brain FMRI and fast diffusion imaging. PLoS One. 2010; 5(12):e15710. [PubMed: 21187930]

8. Kim T, Shin W, Zhao T, Beall EB, Lowe MJ, Bae KT. Whole brain perfusion measurements using arterial spin labeling with multiband acquisition. Magn Reson Med. 2013; 70(6):1653–1661. [PubMed: 23878098]
9. Wang Y, Moeller S, Li X, Vu AT, Krasileva K, Ugurbil K, Yacoub E, Wang DJ. Simultaneous multi-slice Turbo-FLASH imaging with CAIPIRINHA for whole brain distortion-free pseudo-continuous arterial spin labeling at 3 and 7 T. Neuroimage. 2015; 113:279–288. [PubMed: 25837601]
10. Feinberg DA, Beckett A, Chen L. Arterial spin labeling with simultaneous multi-slice echo planar imaging. Magn Reson Med. 2013; 70(6):1500–1506. [PubMed: 24130105]
11. Ghariq E, Chappell MA, Schmid S, Teeuwisse WM, van Osch MJ. Effects of background suppression on the sensitivity of dual-echo arterial spin labeling MRI for BOLD and CBF signal changes. Neuroimage. 2014; 103:316–322. [PubMed: 25280450]
12. St Lawrence KS, Owen D, Wang DJ. A two-stage approach for measuring vascular water exchange and arterial transit time by diffusion-weighted perfusion MRI. Magn Reson Med. 2012; 67(5): 1275–1284. [PubMed: 21858870]
13. Mani S, Pauly J, Conolly S, Meyer C, Nishimura D. Background suppression with multiple inversion recovery nulling: applications to projective angiography. Magn Reson Med. 1997; 37(6): 898–905. [PubMed: 9178242]
14. Coleman, T., Li, Y. On the Convergence of Reflective Newton Methods for Large-scale Nonlinear Minimization Subject to Bounds. Vol. 67. Ithaca, NY, USA: Cornell University; 1994.
15. Coleman TF, Li Y. An interior trust region approach for nonlinear minimization subject to bounds. SIAM Journal on optimization. 1996; 6(2):418–445.
16. Setsompop K, Gagoski BA, Polimeni JR, Witzel T, Wedeen VJ, Wald LL. Blipped-controlled aliasing in parallel imaging for simultaneous multislice echo planar imaging with reduced g-factor penalty. Magn Reson Med. 2012; 67(5):1210–1224. [PubMed: 21858868]
17. Cauley SF, Polimeni JR, Bhat H, Wald LL, Setsompop K. Interslice leakage artifact reduction technique for simultaneous multislice acquisitions. Magn Reson Med. 2014; 72(1):93–102. [PubMed: 23963964]
18. Cunningham CH, Wood ML. Method for improved multiband excitation profiles using the Shinnar-Le Roux transform. Magn Reson Med. 1999; 42(3):577–584. [PubMed: 10467303]
19. Shang H, Larson PE, Kerr A, Reed G, Sukumar S, Elkhaled A, Gordon JW, Ohliger MA, Pauly JM, Lustig M, Vigneron DB. Multiband RF pulses with improved performance via convex optimization. J Magn Reson. 2016; 262:81–90. [PubMed: 26754063]
20. Wang Z, Wang J, Connick TJ, Wetmore GS, Detre JA. Continuous ASL (CASL) perfusion MRI with an array coil and parallel imaging at 3T. Magn Reson Med. 2005; 54(3):732–737. [PubMed: 16086314]
21. Glover GH, Lai S. Self-navigated spiral fMRI: interleaved versus single-shot. Magn Reson Med. 1998; 39(3):361–368. [PubMed: 9498591]
22. Vidorreta M, Wang Z, Rodriguez I, Pastor MA, Detre JA, Fernandez-Seara MA. Comparison of 2D and 3D single-shot ASL perfusion fMRI sequences. Neuroimage. 2013; 66:662–671. [PubMed: 23142069]
23. Duyn JH, Tan CX, van Gelderen P, Yongbi MN. High-sensitivity single-shot perfusion-weighted fMRI. Magn Reson Med. 2001; 46(1):88–94. [PubMed: 11443714]

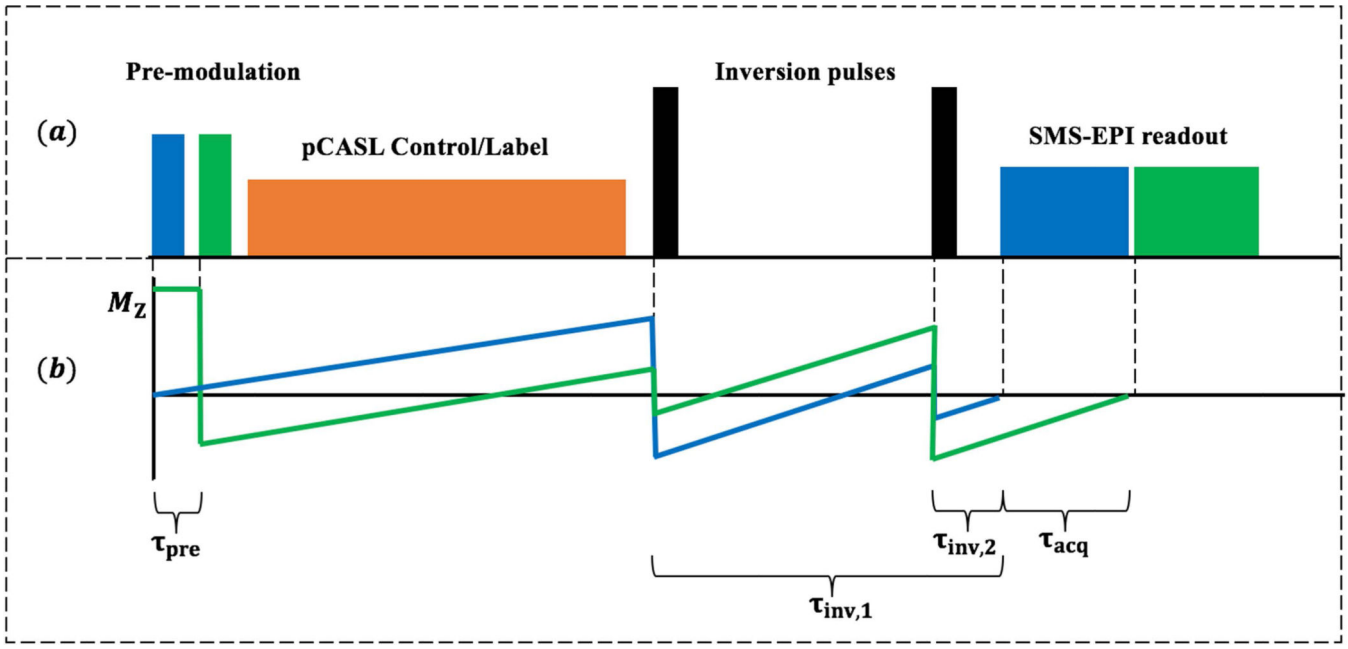

Figure 1.

(a) Illustration of CSD-BS scheme: Slice-dependent pre-modulation pulses with SMS excitation modulates background signal in brain prior to the pCASL labeling train. Two spatially non-selective inversion pulses are placed within the post labeling delay to avoid the interruption of labeling module. SMS-EPI images are acquired sequentially with a 45 ms readout. (b): A two-slice example to demonstrate the trajectory of background signal. Longitudinal signal in each group of slices (blue and green) is modulated separately to reach the nulling point prior to readout of each respectively slice group.

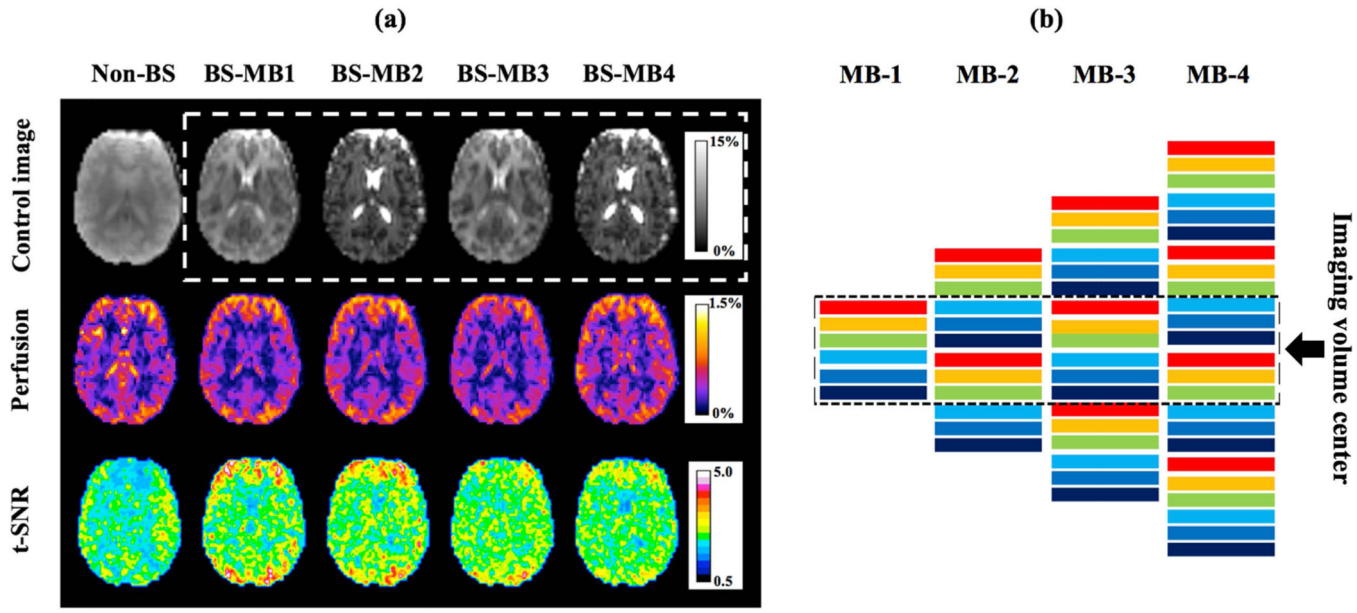

Figure 2.

(a) Results of proposed CSD-BS from one representative slice: row one to three shows control images, perfusion weighted images and t-SNR maps from non-BS SB and CSD-BS MB1/2/3/4 scans. Scale bar in BS and perfusion weighted images indicates the percentage signal relative to average non-BS control signal. (b) Excitation ordering of six slice groups for MB-1/2/3/4 scans. Totally 6/12/18/24 slices were collected with MB factors 1/2/3/4. Slices were sequentially excited following an ascending order and showed different contrast due to BS, as illustrated by different colors. Dashed box indicates the common six slices shared by all MB factors and image contrast was identical for MB-1/3 and MB-2/4 respectively.

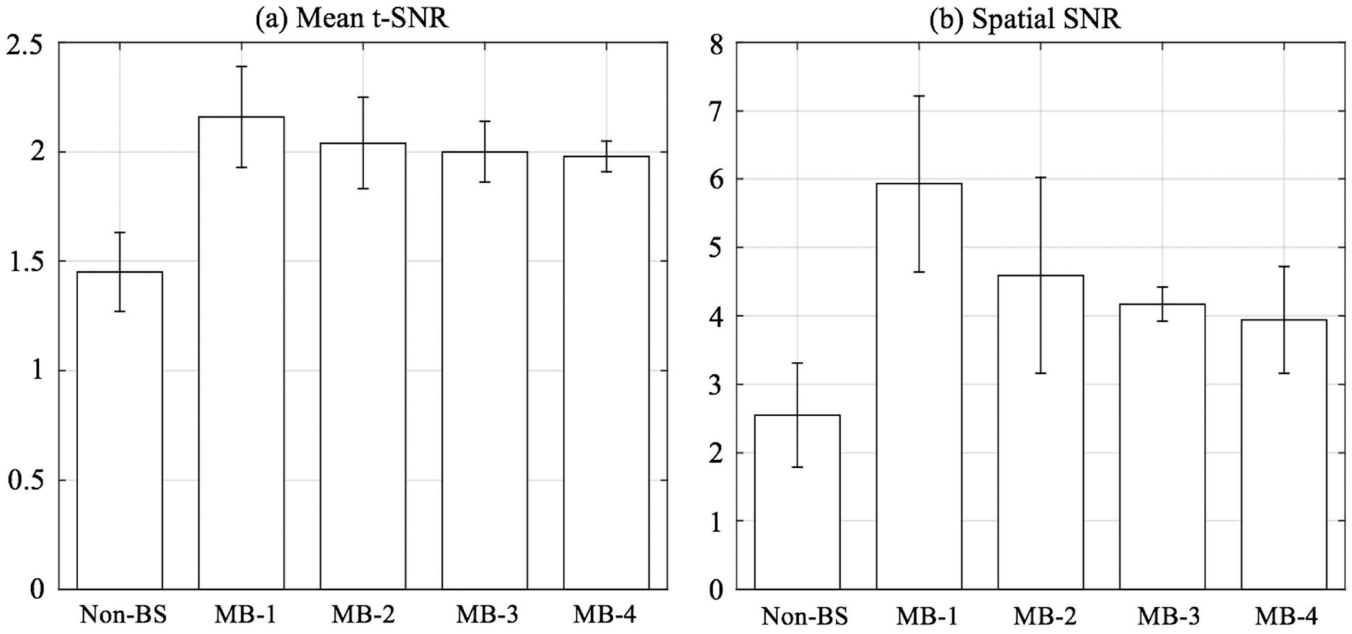

Figure 3.

Mean t-SNR and spatial SNR from non-BS SB and CSD-BS MB scans. Both t-SNR and spatial SNR were calculated in gray matter for common six slices.

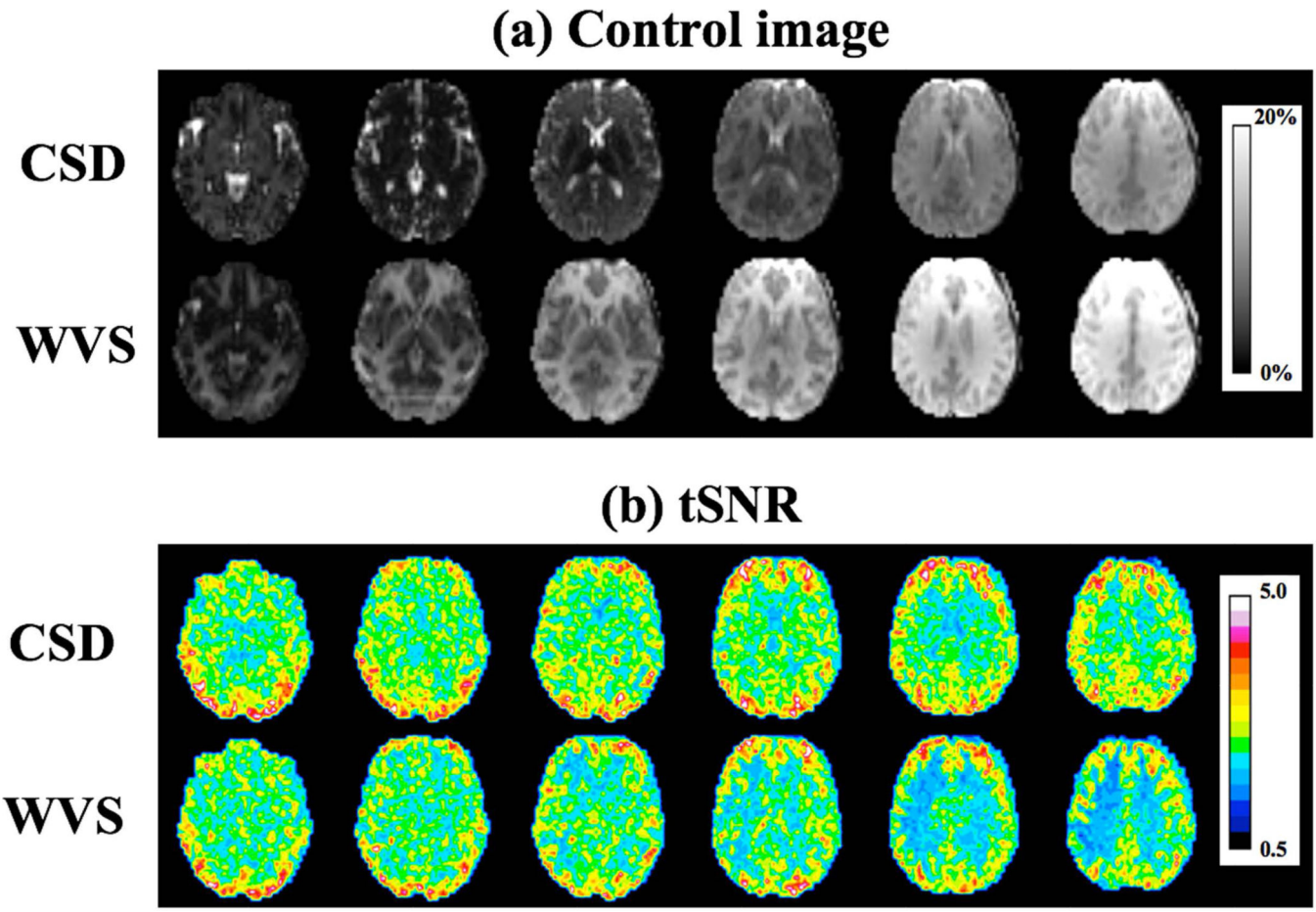

Figure 4.

Comparison between CSD-BS and WVS-BS: (a) Control signal acquired with the two BS schemes. Imaging slices were excited sequentially from left to right and scale bar shows the percentage signal relative to non-BS control signal. (b) Corresponding tSNR maps. Both BS schemes were evaluated on six slices without MB acceleration.

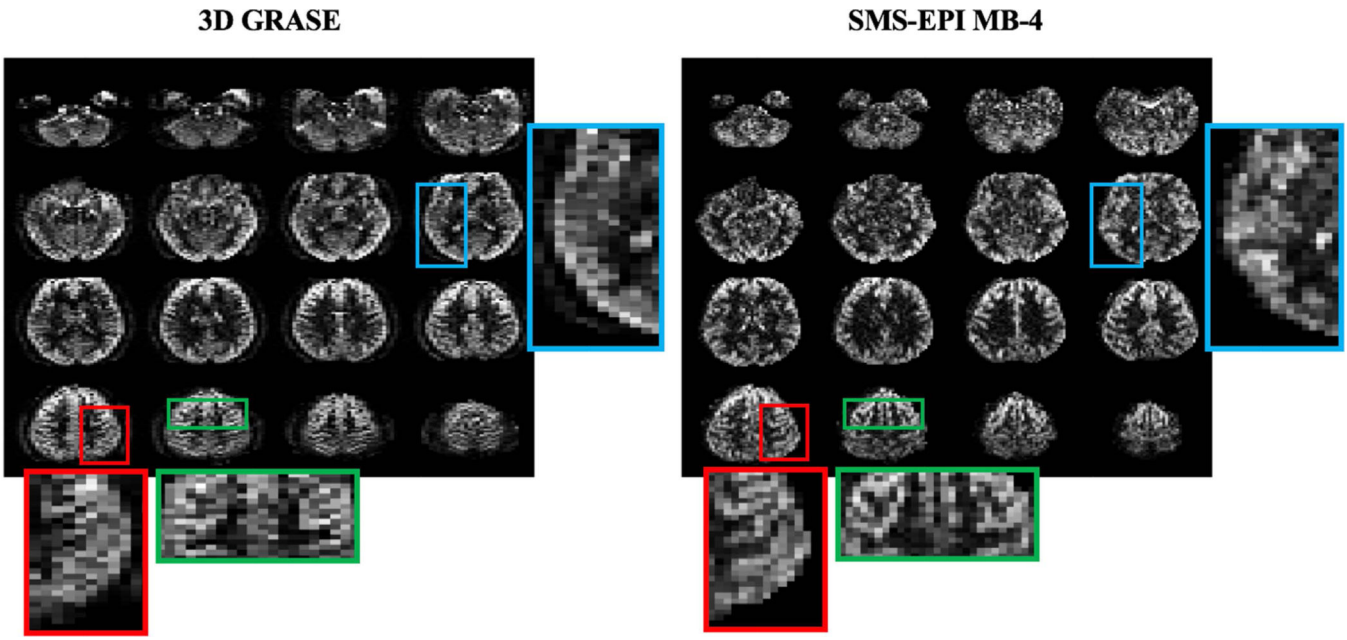

Figure 5.

Perfusion weighted images of central 16 slices from 3D segmented GRASE and SMS-EPI MB-4. For qualitative comparison, even and odd slices in 3D GRASE were added to match the slice position in SMS-EPI scan. Three regions (highlighted by red, green and blue frames) were enlarged for comparison of blurring effects between 3D GRASE and 2D SMS-EPI.